

Two-Dimensional Finite-Difference Time-Domain Method Combined with Open Boundary for Signal Integrity Issues between Isolation Islands

Chun-Te Wu and Ruey-Beei Wu

Dept. of Electrical Engineering and Graduate Institute of Communication Engineering,
National Taiwan University, Taipei, Taiwan, 10617, R.O.C.

Tel: +886-2-23635251 x 340 Fax: +886-2-23638247

E-mail: rbwu@ew.ee.ntu.edu.tw

Abstract

A novel method is proposed to take into account radiation effects due to the open boundary of PCB on ground bounce between isolated power/ground planes by the 2D-FDTD method hybridized with integral equation formulation for the exterior field. An efficient simulation procedure is established by casting equivalent inductances and capacitances with phase retardation into 2D-FDTD. Simulation results for the radiation effects due to open boundary or among isolated power/ground planes are presented and validated by measured data.

1 Introduction

Isolated power or ground areas, so called voltage "islands", are commonly used in PCB to distribute multiple power sources or separate noisy circuit areas. Conventionally, investigation of signal integrity issues at split ground and power planes should be resorted to three-dimensional FDTD method [1]. A lot of computer memory and CPU time is required to perform the simulation. In a PCB, the electric field between ground/power planes is uniform in the longitudinal direction except near the edge due to the fringing effects. A more efficient approach should be based on 2D-FDTD. However, such an approach usually puts perfect magnetic conductor (PMC) on the edge and neglects the radiation effects. A radiation boundary condition suitable for 2D-FDTD has never been proposed before in the literature.

In this paper, a new radiation boundary suitable for 2D-FDTD is developed to solve the signal integrity issues between isolation islands. Through comparison between simulated and measured data, it has been proven to be accurate and efficient.

2 Theory

Consider a patch shown in Fig. 1 in which the ground plane is infinite. The field outside the patch can be expressed by putting equivalent magnetic source $\vec{M} = \vec{E} \times \hat{n}$ along the edge of the patch. If the ground plane is large enough to apply image theory, the ground plane can be replaced by doubling the magnetic current, which is illustrated in Fig. 2. The scattering magnetic field outside the patch due to the magnetic current can be expressed as

$$\vec{H}^s = \frac{\nabla \nabla \cdot \vec{F} + k^2 \vec{F}}{j\omega\mu} \quad (1)$$

$$\vec{F} = \int_{\Gamma} \frac{e^{-jkR}}{4\pi R} 2\vec{M}(\vec{r}') d\vec{r}' \quad (2)$$

where R is the distance between field and source points, k is propagation constant, \vec{F} is magnetic vector potential, and Γ presents the surface along the edge.

Assume that $\vec{M}(\vec{r}')$ is modeled by roof-top bases, as illustrated in Fig. 3. The magnetic currents can be expressed as

$$\vec{M}(\vec{r}') = \sum_j V_j \vec{B}_j(\vec{r}') \quad (3)$$

This work was jointly supported under the Grants 89-E-Fa06-2 by Ministry of Education, and NSC 89-2213 E002-197 by National Science Council, Republic of China.

where $\vec{B}_j(\vec{r}')$ is the roof-top basis on the area of cells $Ce_{j-\frac{1}{2}}$ and $Ce_{j+\frac{1}{2}}$ as illustrated in Fig. 4, and the corresponding unknown coefficient V_j denotes the voltage at the branch S_j .

After some deduction of mathematics, an equivalent circuit model can be obtained. Figure 5 shows the equivalent circuit for updating the voltage at branch S_i . The equivalent circuit equations for this method is given by

$$(C_{FDTD} + C_{ii}) \frac{dV_i}{dt} = I_i^{inc} - I_i^+ + I_i^- - I_i^g - I_{i,i+1} + I_{i-1,i} \quad (5)$$

where $C_{ij} = \varepsilon \int_{\Gamma_i} \int_{\Gamma_j} \frac{e^{-jkR}}{2\pi R} \vec{B}_i(\vec{r}') \cdot \vec{B}_j(\vec{r}') d\vec{r}' d\vec{r}$, and

$$I_i^+ = \sum_{j \neq i} I_{i+\frac{1}{2},j+\frac{1}{2}} = \sum_{j \neq i} \frac{L_{i+\frac{1}{2},j+\frac{1}{2}}^{-1}}{L_{j-\frac{1}{2},j-\frac{1}{2}}^{-1}} I_{j,j+1}^{(t - \frac{|\vec{s}_{i+\frac{1}{2}} - \vec{s}_{j+\frac{1}{2}}|}{c})}$$

$$I_i^- = \sum_{j \neq i} I_{i-\frac{1}{2},j-\frac{1}{2}} = \sum_{j \neq i} \frac{L_{i-\frac{1}{2},j-\frac{1}{2}}^{-1}}{L_{j-\frac{1}{2},j-\frac{1}{2}}^{-1}} I_{j-1,j}^{(t - \frac{|\vec{s}_{i-\frac{1}{2}} - \vec{s}_{j-\frac{1}{2}}|}{c})}$$

$$I_i^g = \sum_{j \neq i} j\omega C_{ji} V_j = \sum_{j \neq i} C_{ji} \frac{d}{dt} V_j^{(t - \frac{|\vec{s}_j - \vec{s}_i|}{c})}$$

The governing equation for $I_{i,i+1}$ is

$$L_{i+\frac{1}{2},j+\frac{1}{2}} \frac{d}{dt} I_{i,i+1} = V_i - V_{i+1} \quad (6)$$

where $L_{i+\frac{1}{2},j+\frac{1}{2}}^{-1}$ is the average of $\frac{e^{-jkR}}{2\pi\mu R}$ over cells $Ce_{i+\frac{1}{2}}$ and $Ce_{j+\frac{1}{2}}$.

The physical meaning of coupling capacitance C_{ji} is the capacitive coupling from branch voltage V_j to branch voltage V_i , C_{ii} is the self-capacitance for the branch V_i , and $L_{i+\frac{1}{2},j+\frac{1}{2}}$ is the self-inductance at cell $Ce_{i+\frac{1}{2}}$. In time domain, the effects of C_{ij} and $L_{i+\frac{1}{2},j+\frac{1}{2}}^{-1}$ happens at $\frac{|\vec{s}_i - \vec{s}_j|}{c\Delta t}$ time steps later, due to the phase retardation term e^{jkR} , where \vec{s}_i means the position vector at the center of S_i .

3 Simulation Results

A structure of two isolation power islands is fabricated to investigate the coupling between islands. As in Fig. 6, the separation of the two isolation is 1mm, the thickness of substrate is 1.2mm, and the dielectric constant of substrate $\varepsilon_r = 4.2$. The whole structure is symmetric. There are no vias or transmission lines between these two patches. The noise, if generated, could be contributed to the other island.

In the experiment, a ramped step pulse of about amplitude 0.25 volts and rise time 100ps is used as the excitation on port 1. The TDR and TDT signals at point 1 and 2, respectively, are measured by Tektronix 11801C. The measured input waveform is used as the excitation signal in numerical simulation. Figures 7 shows the results at TDR port by simulation and experiment. In the case of PMC boundary, the RC time constant is found to be approximate 1162ps, if the capacitance is calculated from patch area A and substrate thickness d by parallel-plate formula $C = \varepsilon \frac{A}{d} \approx 23.24 pF$, and the resistance R is internal resistor of 50 ohm. The RC time constant is larger in the present method, since the fringing effect enlarges the effective area of patch. It is noted from the figure that the RC time constant of

experiment is even longer due to the loss of measurement system and PCB.

As for TDT shown in Fig. 8, the coupling noise level at port 2 is measured to be 4mV as compared to the simulated value of 5.3mV by the present method. In other words, the generated coupled noise by isolation islands in the present case may achieve about 2% of the input level. The over-estimation in the simulated level can be contributed to the negligence of substrate and conductor loss.

Figure 9 shows the power spectrum density of the measured and simulated waveforms. Due to the position of excitation, the first two peaks should occur at TM_{10} at 2.375GHz, and TM_{20} at 4.714GHz. The agreement between measurement and simulation demonstrates the accuracy of the present method.

4 Conclusions

A new methodology is presented in this paper to simulate the signal integrity issues between isolation islands due to radiation coupling. The methodology can be cast into 2D-FDTD to analyze the radiation problems of PCB. Numerical and experimental results have both demonstrated the accuracy of this method. Although the coupled noise caused by radiation is less than 2%, the effects may severely deteriorate the signal integrity of other islands at some resonant frequencies.

5 References

- [1] H. J. Liaw and H. Merkelo, "Signal integrity issues at split ground and power planes," *Proceedings of 46th IEEE Electronic Components and Technology Conference*, 1996, pp. 752 –755.

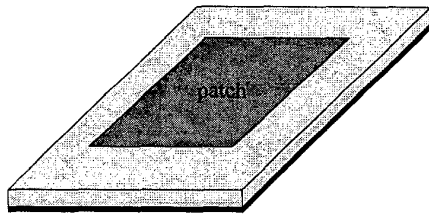


Figure 1 A patch on a large substrate and ground plane.

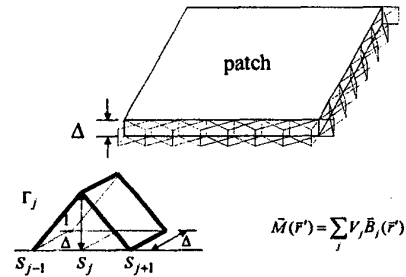


Figure 3 Using roof-top bases to expand magnetic currents.

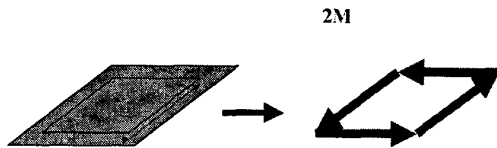


Figure 2 Applying equivalent principle and image theory to the boundary of edges

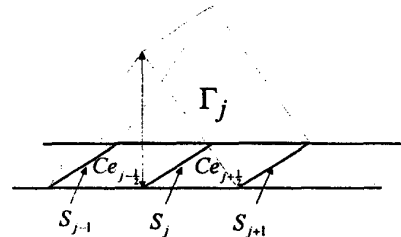


Figure 4 An illustration to explain the branch Br_j and cell $Ce_{j+\frac{1}{2}}$.

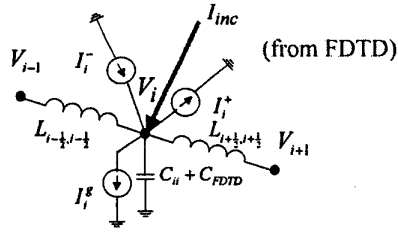


Figure 5 Equivalent circuit for updating the voltage at branch Br_i .

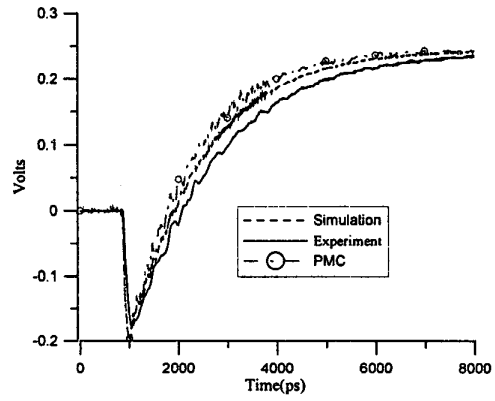


Figure 7 Measured and simulated waveforms of the TDR signal on port 1.

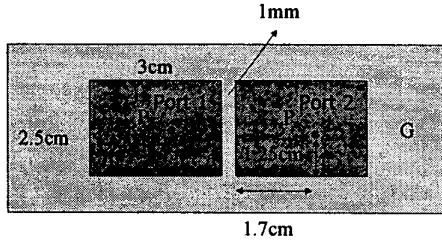


Figure 6 A test PCB of isolation power plane used for experiment and simulation.

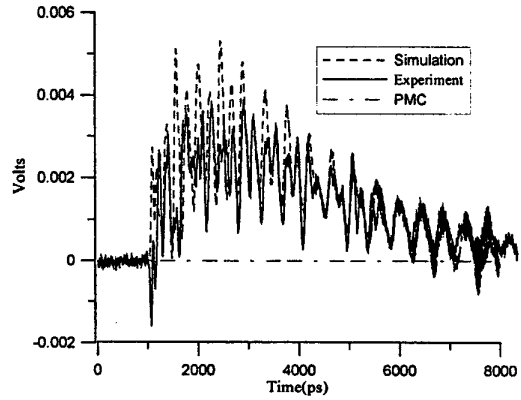


Figure 8 Measured and simulated waveforms of the TDT signal on port 2.

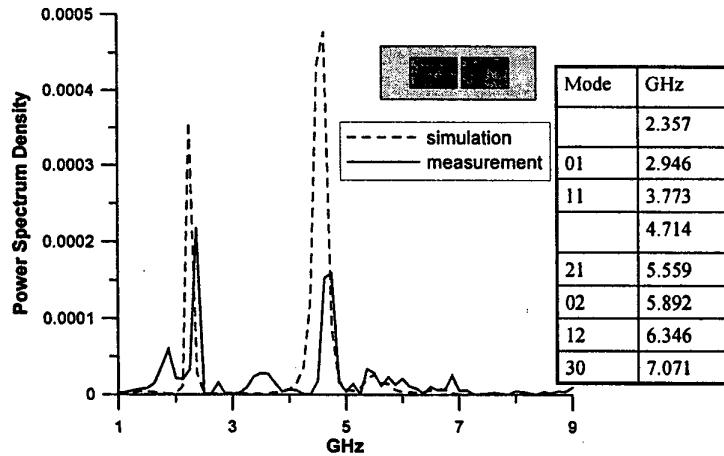


Figure 9 Power spectrum density of TDT for simulated and measured